



Hydroxylated 2-Ethylhexyl tetrabromobenzoate isomers in house dust and their agonistic potencies with several nuclear receptors[☆]



Hui Peng^a, Jianxian Sun^{a, *}, David M.V. Saunders^a, Garry Codling^a, Steve Wiseman^a, Paul D. Jones^{a, b}, John P. Giesy^{a, c, d, e, f, g}

^a Toxicology Centre, University of Saskatchewan, 44 Campus Drive, Saskatoon, SK, S7N 5B3, Canada

^b School of Environment and Sustainability, 117 Science Place, Saskatoon, SK, S7N 5C8, Canada

^c Department of Veterinary Biomedical Sciences, University of Saskatchewan, Saskatoon, SK, S7N 5B3, Canada

^d Zoology Department, Center for Integrative Toxicology, Michigan State University, East Lansing, MI, USA

^e Department of Biology and Chemistry, City University of Hong Kong, Kowloon, People's Republic of China

^f School of Biological Sciences, University of Hong Kong, People's Republic of China

^g State Key Laboratory of Pollution Control and Resource Reuse, School of the Environment, Nanjing University, Nanjing, People's Republic of China

ARTICLE INFO

Article history:

Received 9 February 2017

Received in revised form

28 April 2017

Accepted 29 April 2017

Available online 13 May 2017

Keywords:

Brominated flame retardants

OH-TBB

Firemaster[®] 550

BZ-54

PPAR γ

ABSTRACT

In the current study, by combining ultra-high resolution (UHR) MS¹ spectra, MS² spectra, and derivatization, three hydroxylated isomers of 2-ethylhexyl tetrabromobenzoate (OH-TBB) were identified in Firemaster[®] 550 and BZ-54 technical products. Also, a new LC-UHRMS method, using atmospheric pressure chemical ionization (APCI), was developed for simultaneous analysis of OH-TBB, TBB, hydroxylated bis(2-ethylhexyl)-tetrabromophthalate (OH-TBPH) and TBPH in 23 samples of dust collected from houses in Saskatoon, SK, Canada. OH-TBBs were detected in 91% of samples, with a geometric mean concentration of 0.21 ng/g, which was slightly less than those of OH-TBPH (0.35 ng/g). TBB was detected in 100% of samples of dust with a geometric mean concentration of 992 ng/g. Significant ($p < 0.001$) log-linear relationships between concentrations of OH-TBBs, TBB, or OH-TBPHs and TBPH in dust support the hypothesis of a common source of these compounds. OH-TBBs were found to be strong agonists of peroxisome proliferator-activated receptor gamma (PPAR γ) and weaker agonists of the estrogen receptor (ER), but no agonistic potencies was observed with the androgen receptor (AR). Occurrence of OH-TBBs in technical products and house dust, together with their relatively strong PPAR γ potencies, indicated their potential risk to health of humans.

© 2017 Elsevier Ltd. All rights reserved.

1. Introduction

There is concern among regulatory agencies and the general public about environmental persistence, bioaccumulation and toxicities of brominated flame retardants (BFRs) (Alaee and Wenning, 2002). Until recently polybrominated diphenyl ethers (PBDEs) were the most widely used BFRs (Birnbaum and Staskal, 2004). However, due to concerns regarding their ubiquitous presence in the environment (Chen and Hale, 2010; Chen et al., 2012; Kohler et al., 2008; Lake et al., 2011; Leung et al., 2007; Xie et al., 2011), trophic magnification in food webs (Wan et al., 2008;

Wolkers et al., 2004), and toxic potencies (Alm et al., 2010; Hakk and Letcher, 2003; Muirhead et al., 2006; Zhou et al., 2001), starting in 2004, sale of two major commercial formulations of PBDEs, penta- and octa-BDE, were voluntary withdrawn or banned in some parts of the world (Ma et al., 2013). Since protection against inflammability of products was still needed, and in fact mandated in many jurisdictions, to replace PBDEs and other BFRs, alternative brominated compounds, often termed novel brominated flame retardants (NBFRs) were developed and used. Therefore, investigations of concentrations and distribution of these compounds in the environment are required to assess any potential risks these compounds pose to humans or wildlife.

Firemaster[®] 550 (FM-550) and Firemaster[®] BZ-54 (BZ-54), both of which contain 2-ethylhexyl-2,3,4,5-tetrabromobenzoate (TBB) and bis(2-ethylhexyl)-tetrabromophthalate (TBPH), are commercial mixtures used as replacements for PBDEs (Ma et al., 2012). FM-

[☆] This paper has been recommended for acceptance by Dr. Chen Da.

* Corresponding author.

E-mail address: sunsjx@gmail.com (J. Sun).

550 consists of approximately 35% TBB and 15% TBPH, and BZ-54 consists of approximately 70% TBB and 30% TBPH (Barr et al., 2010). Because of their potentials to disrupt normal functions of the endocrine system, concerns are emerging regarding health risks of TBB and TBPH (Saunders et al., 2013). For example, a mono-ester metabolite of TBPH interacts with the peroxisome proliferator activated receptor γ (PPAR γ) and pregnane X receptor (PXR) (Skledar et al., 2016; Springer et al., 2012), and both TBB and TBPH have antagonistic activities on several nuclear receptors, *in vitro* (Klopčič et al., 2016; Saunders et al., 2013). In addition to potential toxicities, studies have reported widespread presence of TBB and TBPH in house dust (Hoffman et al., 2014; Stapleton et al., 2008, 2014), air (Moller et al., 2011; Vorkamp et al., 2015) and sediment (Klosterhaus et al., 2012; Liu et al., 2014). Recently, two novel hydroxylated by-products of TBPH (OH-TBPH) (Fig. 1), were identified in FM-550 and BZ-54, and in samples of house dust by use of a liquid chromatography (LC)-Q Exactive method (Peng et al., 2015). Compared to TBPH, TBB has a smaller log K_{OW} (8.8) and is expected to have greater bioaccessibility and thus potential for adverse effects to health of humans (Fang and Stapleton, 2014; Saunders et al., 2013). There is evidence that people are exposed to TBB as indicated by the detection of TBB in blood serum of humans (Zhou et al., 2014), and the metabolite of TBB, tetrabromobenzoic acid (TBBA), has been observed in urine from humans (Butt et al., 2014; Hoffman et al., 2014). Because the sources of emission of TBPH and TBB are similar, it is likely that hydroxylated by-products of TBB also exist in FM-550 and BZ-54, and house dust.

Compounds with phenol groups sometimes have greater biological activities than their non-hydroxylated analogues (Fang et al., 2015a; Mercado-Feliciano and Bigsby, 2008; Riu et al., 2011). For example, compared to PBDEs, hydroxylated PBDEs (OH-PBDEs) are more potent activators of the estrogen receptor (ER) (Mercado-Feliciano and Bigsby, 2008). Activation of ER is a well-known mechanism of action of phenolic compounds of approximately 14 Å with para-OH moieties that are similar in conformation to 17 β -estradiol (E2). Estrogenic compounds can interfere with functions of endocrine systems and cause deleterious effects on humans and wildlife including reproductive impairment, hormonal cancers, and obesity (Grun and Blumberg, 2007; Jenkins et al., 2009; Newbold et al., 2009). Halogenated phenols could also potentially activate PPAR γ , exemplified by OH-PBDEs and tetrabromobisphenol A (TBBPA) (Fang et al., 2015a; Riu et al., 2011). In particular, the combination of van der Waals interaction of halogen atoms and hydrogen bonds of phenolic group are both necessary to fit into the binding pocket of PPAR γ (Riu et al., 2011). Therefore, assessment of

the potential for OH-TBBs to act as agonists of nuclear receptors, especially ER and PPAR γ , is important to assess their potential risks to health of humans and the environment.

The goal of the current study was to investigate potential occurrence of OH-TBB in two technical mixtures of flame retardants (FM-550 and BZ-54) and samples of dust. This was accomplished by improvement of a previously developed method based on the LC-Q Exactive ultra-high resolution mass spectrometer (UHR-MS), which used atmospheric pressure chemical ionization (APCI) for simultaneous analysis of OH-TBB, OH-TBPH, TBPH and TBB in samples of dust. Agonistic potentials of TBB and OH-TBB on multiple receptors including ER, PPAR γ , and androgen receptor (AR) were evaluated by *in vitro* cellular assays.

2. Materials and methods

2.1. Chemicals and reagents

Details are provided in Supporting Material.

2.2. Collection of dust

Twenty-three samples of dust were collected from 8 houses (2–3 samples per house) across Saskatoon, SK, Canada from May to August 2013. Dust was collected in a cellulose extraction thimble (Whatman International, Pittsburgh, PA, USA) attached to a Eureka Mighty-Mite vacuum cleaner (model 3670) (Allen et al., 2008; Stapleton et al., 2008). The extraction thimble was inserted between the vacuum tube extender and suction tube, and was secured by use of a metal hose clamp. Extraction thimbles were Soxhlet-extracted with DCM for 2 h prior to use. The equivalent of the entire floor area was sampled in each room. All sampling components upstream of the extraction thimble were cleaned after each sampling event. Prior to the sample pretreatment, non-dust particles, such as hair, were removed.

2.3. Sample pretreatment

Samples were processed with a liquid extraction method followed by Florisil solid phase extraction (SPE) cleanup, as described in our previous studies (Peng et al., 2015, 2016) and Supporting Material.

2.4. Derivatization with dansyl chloride (DNS)

Reaction of OH-TBBs with DNS was conducted in a sealed 1.5 mL glass sample vial (Waters, Milford, MA, USA). Aliquots of stock solution (50 μ L of 10 mg/L OH-TBBs in acetone) were added to 1.5 mL sample vials followed by 100 μ L of DNS in acetone (5 mg/mL), 300 μ L of sodium carbonate (0.1 M), and 380 μ L of acetone, and were shaken vigorously for 1 min. The resulting mixture was incubated at 65 $^{\circ}$ C for 10 min, then vortexed for 30 s. The reaction solution was used directly for ultra performance liquid chromatography (UPLC) Q Exactive analysis.

2.5. Instrumental analysis

Aliquots of extracts were analyzed by use of a Q Exactive mass spectrometer equipped with a DionexTM UltiMateTM 3000 UHPLC system (Thermo Fisher Scientific). Data were acquired by use of one full scan mode, followed by two selected ion monitoring (SIM) with an APCI ionization source. Full scan mode was used to record all the MS¹ information for future retrospective data analysis, but SIM mode was used to monitor the four target compounds to expand dynamic range. Details of instrument conditions were provided in

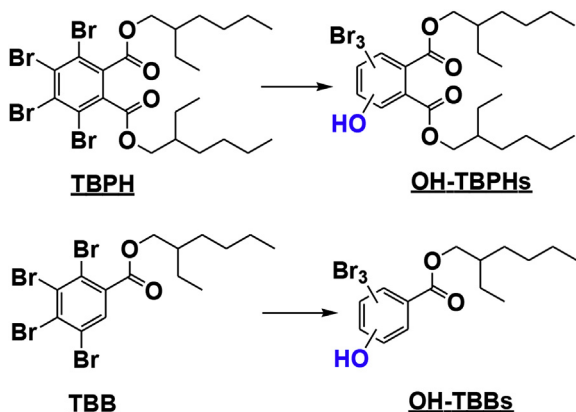


Fig. 1. Structures of TBPH, OH-TBPH isomers, TBB and OH-TBB isomers.

Supporting Material.

2.6. Quality assurance/quality control

Because minor contamination of TBPH was detected during the processing of samples and in cellulose extraction thimbles (mean value was 0.33 ng/g), procedural blanks were processed with each batch of 10 samples. Background contamination was not detected for TBB, OH-TBPH or OH-TBB. Standards were re-injected after every four to six sample injections, and acetone was injected after each standard to monitor potential carryover contamination. Due to minor background contamination of TBPH, the detection of limit (LOD) was defined as three times the mean background signals from 3 procedural blanks, and was 1.1 ng/g for TBPH. The LODs for other chemicals were defined as three times the noise, and were 0.02, 0.02 and 3.0 ng/g for OH-TBPH, OH-TBB and TBB in dust, respectively. Recoveries were determined by spiking standards to samples of dust ($n = 3$) prior to extraction. The dust sample (dust-23) with the lowest concentration of TBPH and TBB was selected for recovery experiments. Spiked concentrations were 500 ng/g TBPH, 500 ng/g TBB, 10 ng/g OH-TBPH and 10 ng/g OH-TBB, which were at least three times greater than respective concentrations of these isomers in dust-23. Recoveries from dust were 88 ± 13 , 79 ± 9.0 , 74 ± 17 and $86 \pm 9.1\%$, for TBPH, TBB, OH-TBPH and OH-TBB, respectively. Quantification of TBB was adjusted for recoveries by use of internal standard d_{17} , $^{13}\text{C}_6$ -TBB, for which recoveries in dust averaged at $84 \pm 25\%$. Concentrations of OH-TBB were quantified by use of purified OH-TBB standards. Because the three isomers of OH-TBB could not be separated from the purified standards, the total peak abundance of the three isomers were used for quantification. Concentrations of OH-TBB were calculated without use of an internal standard due to the lack of commercial internal standards and because recoveries were $>80\%$ and stable across replicate recovery samples. Calibration curves showed strong linearity with $r^2 > 0.99$ for all four target chemicals (Fig. S1), during the concentration series of 0, 0.097, 0.195, 0.391, 0.781, 1.563, 3.125, 6.25, 12.5, 25 and 50 ng/mL.

2.7. Nuclear receptor (ER, PPAR γ and AR) agonistic activity test

Nuclear receptor potencies of OH-TBB or TBB were tested using *in vitro* cell reporter systems. Particularly, ER potency was tested by use of the MCF-7 human breast carcinoma cell line stably transfected with an ER-controlled luciferase reporter gene construct (MVLN). PPAR γ potencies was tested by use of the human PPAR γ reporter assay kit. AR potencies was tested by use of the MDA-kb2 cell reporter system (ATCC CRL-2713). Details of cell culture and treatment are provided in Supporting Material.

2.8. Analysis of data

Statistical analyses were conducted by use of SPSS software (SPSS Inc, V.19). Values less than LOD were replaced by a value equivalent to the LOD/2. Frequency distributions of chemical concentrations were assessed to see if they could be described by the normal probability distribution by use of the Shapiro-Wilk test, and data were log-transformed if necessary to more closely approximate the normal distribution before application of log linear regression analysis and *t*-test. Considering that sources and profiles of chemicals might be different between rooms in a house, all 23 dust samples from eight homes were treated equally as independent samples and were included in the log-regression analysis. Differences with $p < 0.05$ were considered significant.

To clarify the potential sources of target chemicals, fractions of TBB (f_{TBB}) and OH-TBB ($f_{\text{OH-TBB}}$) (Equations (1) and (2)), and

percentages of OH-TBB ($P_{\text{OH-TBB}}$) and OH-TBPH ($P_{\text{OH-TBPH}}$) to native compounds were calculated (Equations (3) and (4)).

$$f_{\text{TBB}} = \frac{[\text{TBB}]}{[\text{TBB}] + [\text{TBPH}]} \quad (1)$$

$$f_{\text{OH-TBB}} = \frac{[\text{OH-TBB}]}{[\text{OH-TBB}] + [\text{OH-TBPH}]} \quad (2)$$

$$P_{\text{OH-TBB}} = \frac{[\text{OH-TBB}]}{[\text{OH-TBB}] + [\text{TBB}]} \quad (3)$$

$$P_{\text{OH-TBPH}} = \frac{[\text{OH-TBPH}]}{[\text{OH-TBPH}] + [\text{TBPH}]} \quad (4)$$

where: [TBB], [TBPH], [OH-TBB], and [OH-TBPH] represent the concentrations of corresponding chemicals.

EC₅₀ of OH-TBB was not determined in the present study, considering the weak estrogenic activities of OH-TBB or the maximum achievable response of PPAR γ potencies is different between OH-TBBs and rosiglitazone. To compare the relative potency (ReP) between compounds, the lowest observed effects concentration (LOEC) was used as previously described for weak agonists (Villeneuve et al., 2000).

$$\text{ReP} = \text{LOEC}_{\text{test}} / \text{LOEC}_{\text{posi}} \quad (5)$$

where LOEC_{test} is the LOEC of tested compounds, LOEC_{posi} is the LOEC of positive controls of corresponding nuclear receptors.

The total equivalents (TEQ_{PPAR γ}) of OH-TBB and TBB were calculated by multiplying their measured concentrations by the corresponding ReP values.

3. Results and discussion

3.1. Detection and confirmation of OH-TBB in technical products

Isomers of OH-TBBs were identified in FM-550 and BZ-54 technical products, which is consistent with the results of a previous study where isomers of OH-TBPH were identified in these technical products (Peng et al., 2015). Three peaks, (a), (b) and (c) were observed that were distinct from the peak associated with TBB (d) in FM-550 and BZ-54 when ions were extracted at m/z 482.8806 (10 parts per million (ppm) window) from full scan mass spectra (200–2000 m/z) in negative ion mode (Fig. 2A and B). Based on full scan mass spectra, values for m/z of the three peaks were 482.8810, 482.8810 and 482.8815, (mass errors of 0.8, 0.8 and 1.9 ppm, respectively) (Fig. 2C) compared to the theoretical m/z value of OH-TBB (482.8806) ([OH-TBB-H]⁻, C₁₅H₁₈O₃Br₃). Based on results of UHR-MS spectra data and the isotopic distribution pattern, the three peaks were expected to be hydroxylated isomers of TBB (Fig. 1). Similar to OH-TBPH, peaks of OH-TBB isomers were eluted from the HPLC column earlier (5.2, 5.4 min and 5.6 min) when 0.1% NH₄OH was used as an additive in methanol compared to pure methanol (~8.1 min without good separation, Fig. S2). These results confirmed that the three peaks were acidic compounds, because their retentions on C18 columns were reduced when basic mobile phases were used. To further confirm the structure of OH-TBB, UHR MS² spectra ($R = 35,000$ at m/z 200) was analyzed in negative ion mode at 30–50 eV collision energies. Several product ions with m/z of 78.9171, 245.1184 and 328.7633 were observed (Fig. 2D). Structures of the product ions were evaluated based on elemental composition with mass error of 15 ppm, 2.4 ppm and -0.6 ppm, respectively. An addition of a hydroxyl substituent

to the aromatic ring was evident for 2 predominant fragments. The fragmentation patterns of OH-TBB were similar to that of OH-TBPH (Peng et al., 2015), since de-bromination and cleavage of an alkyl side-chain were the major routes of fragmentation.

Different from OH-TBPH, for which the sodium adduct was detected in positive ion mode, which provides strong evidence to confirm the molecular ion of OH-TBPH, the sodium adduct of OH-TBB was not detected. Thus, to avoid the possibility that addition of the hydroxyl group was due to a substitution reaction during the process of negative ionization, which has been reported previously for brominated compounds (Kato et al., 2009), DNS was used to further confirm the phenol group of OH-TBB. DNS has been shown to react specifically with phenol and amino group in aqueous solution (Chang et al., 2010; Loukou and Zotou, 2003) while reacting with hydroxyl group under harsh conditions with catalyst (Peng et al., 2013). The dansylated derivative of OH-TBB was observed and was eluted at 10.98 min when using 0.1% formic acid in methanol as the mobile phase (Fig. 2E). Mass spectra showed that the m/z value of the dansylated OH-TBB was 717.9453 with mass error of -2.6 ppm from the theoretical value ($m/z = 717.9473$) (Fig. 2F). Unexpectedly, a single peak representing DNS-OH-TBB was detected. This result might be due to poor separation of the

OH-TBB isomers following dansylation of the chemicals, a process which would have increased hydrophobicity and decreased separation efficiency of the molecules on the C18 column (Szarka et al., 2013). Based on information from multiple lines of experimentation reported here, the final structures of OH-TBBs were presented in Fig. 1.

Three OH-TBB isomers were detected in both BZ-54 and FM-550, which along with another flame retardant mixture DP-54 are major sources of emission of TBPH and TBB (Ma et al., 2012). However, relative contributions of each OH-TBB isomer were different between BZ-54 and FM-550. Relative contributions of OH-TBB1, OH-TBB2 and OH-TBB3 (named by order of elution from the HPLC column) to total OH-TBB&TBB were 0.1, 0.3 and 0.4% in FM-550 (Fig. 2A). Relative contributions of OH-TBB1 (0.1%) and OH-TBB2 (0.3%) in BZ-54 were similar to those of FM-550, but the relative contribution of OH-TBB3 was greater in BZ-54 (0.9%) than FM-550 (Fig. 2B). The relative contribution of total OH-TBBs were 5-fold lower than those of total OH-TBPHs in the same technical products samples (6.3% and 8.0% for total OH-TBPHs in FM-550 and BZ-54 technical products respectively) (Peng et al., 2015). The relatively small percentage of OH-TBB observed might be due to the different synthetic route of TBB from TBPH, as such, an

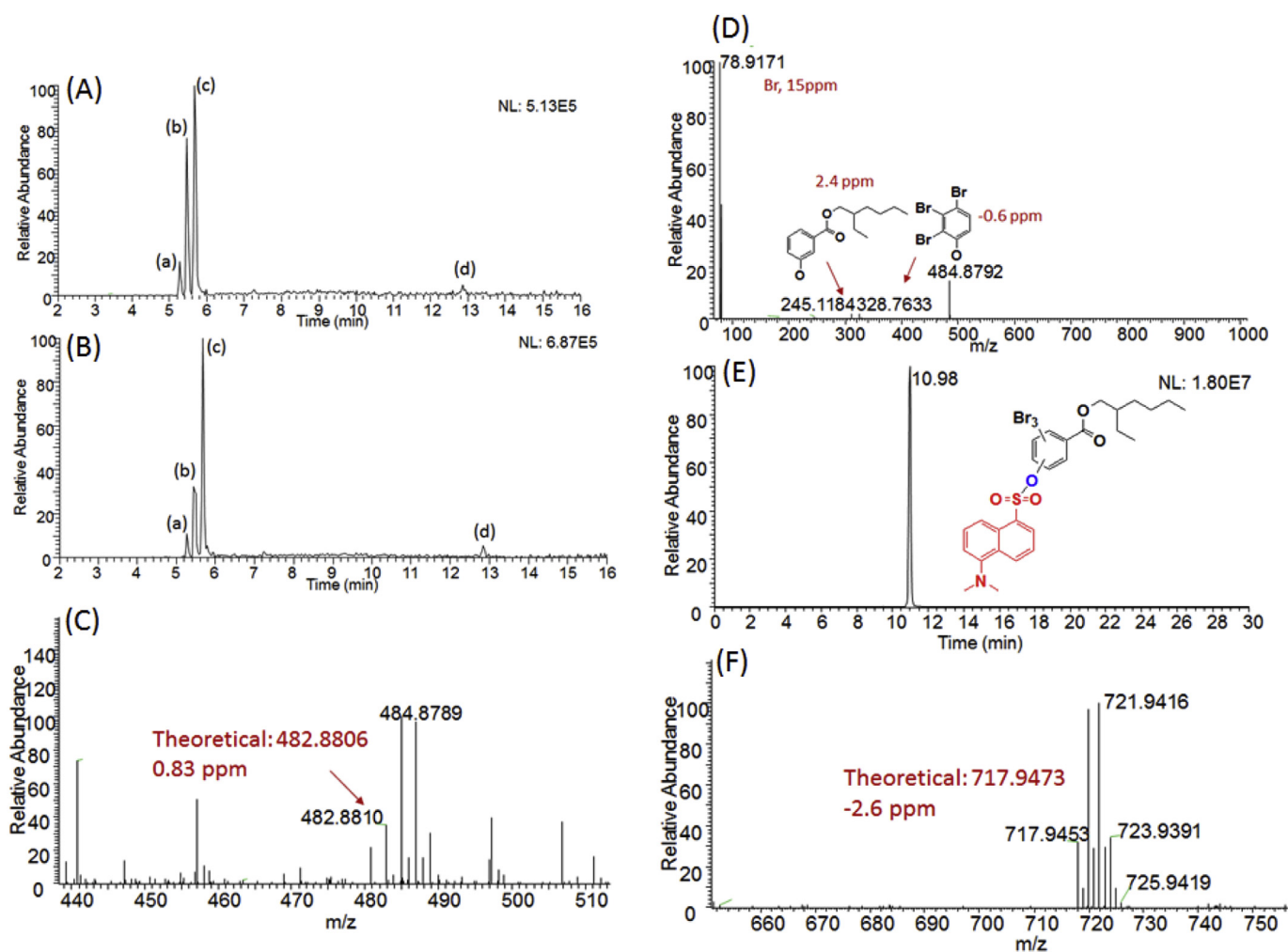


Fig. 2. Chromatogram of extracted ions with m/z 482.8806 (10 ppm window) for FM-550 technical product (A) and BZ-54 technical product (B), determined by use of Q Exactive in APCI (-). (C) Mass spectra of OH-TBB. (D) Product ion mass spectra of OH-TBB at m/z 482.8815. (E) Chromatogram of dansylated OH-TBB. (F) Mass spectra of dansylated OH-TBB. (a) OH-TBB1; (b) OH-TBB2; (c) OH-TBB3; (d) TBB.

investigation of hydroxylated byproducts during the synthetic routes would be interesting to clarify the source of OH-TBB and OH-TBPH.

3.2. Development of analytical method to simultaneously quantify TBPH, TBB, OH-TBPH and OH-TBB in dust

A LC-Q Exactive method using an electrospray ionization source (ESI) was developed previously for analysis of OH-TBPH and TBPH (Peng et al., 2015), which was 200–300-fold more sensitive compared to use of GC-MS (2.5 µg/L) (Springer et al., 2012). However, this method could not detect TBB at concentrations as great as 1 mg/L by use of either ESI (–) or ESI (+) (data not shown), which indicated poor ionization of TBB with ESI. Because APCI has been used previously for analysis of brominated compounds (Zhou et al., 2010), it was used in the current study for detection of TBB. Sensitivity of APCI for detecting OH-TBPH and TBPH was similar (difference was <2 fold) to ESI when 0.1% NH₄OH in methanol was used as the mobile phase (Table 1). Although using APCI (–) instead of ESI (–) as the ionization technique resulted in 5-fold lesser sensitivity of detection when monitoring the ion of OH-TBB ($m/z = 484.8789$), the sensitivity increased greatly when the de-brominated ion [OH-TBB-H-Br][–] was monitored ($m/z = 404.9526$). Based on APCI (–), the instrumental detection limit (IDL) of OH-TBB was 0.006 µg/L, comparable to those of ESI (–) (0.008 µg/L). Most importantly, TBB was successfully detected by use of APCI (–), with an IDL of 0.83 µg/L. Consistent with a previous study (Zhou et al., 2010), a displacement reaction was actually observed for TBB, and [TBB-Br + O][–] was used as the monitoring ion ($m/z = 484.8789$) (the ionization routes of OH-TBPH, OH-TBB and TBB in APCI (–) were shown in Fig. S4). Although sensitivity of the method for detection of TBB was 50-fold lesser than that for OH-TBB, OH-TBPH and TBPH, the sensitivity was adequate to detect TBB in house dust because concentrations of TBB were typically greater than 100 ng/g (Hoffman et al., 2014). Finally, a UPLC-APCI-Q Exactive method was established for simultaneous analysis of OH-TBB, OH-TBPH, TBB and TBPH in both APCI(–) and APCI(+); their typical chromatograms were shown in Fig. 3A. The LC method developed in the current study has greater sensitivity and versatility compared to use of current GC-MS methods as it has lower IDLs and would facilitate simultaneous analysis of polar metabolites such as TBBA.

A two-step extraction method combined with Florisil cartridge cleanup, based on a method described previously (Peng et al., 2015), was used for simultaneous analysis of OH-TBB, TBB, OH-TBPH and TBPH in samples of dust. While TBB was eluted in the DCM fraction from Florisil cartridges, OH-TBBs were eluted separately in the methanol:DCM (v/v, 1:1) fraction (Fig. S5). To assess potential matrix effects, 1000 µg/L of TBPH and TBB and 10 µg/L of OH.

TBPH and OH-TBB were spiked to final extracts (n = 3) before Q Exactive analysis. The signal suppression for all compounds was small, and was 6.1 ± 9.7%, –7.6 ± 5.1%, –8.1 ± 8.0% and –9.3 ± 10%

for OH-TBB, OH-TBPH, TBB and TBPH, respectively.

The developed method was used initially to determine concentrations of TBB and TBPH in a standard reference material of indoor dust (SRM 2585; NIST). Concentrations of TBB and TBPH were determined to be 35.4 and 495 ng/g, respectively. These results were similar to concentrations reported previously (35.2 and 545 ng/g for TBB and TBPH) (Hoffman et al., 2014). Consistent with low concentrations of TBB in the dust, OH-TBB isomers were not detected in SRM 2585, while OH-TBPH2 was detected with a relatively great concentration of 14.8 ng/g.

3.3. Concentrations and profiles of OH-TBB and TBB in dust

The presence of three OH-TBB isomers in both FM-550 and BZ-54 suggests these compounds might have been released to the environment. Therefore, the newly developed method from this study was applied to detect and quantify OH-TBB and TBB in the 23 samples of house dust, and two of the three OH-TBB isomers were detected in 21 of the 23 samples (detection frequency was 91%) (Fig. 3B). The first isomer of OH-TBB (OH-TBB1) was not detected, which might be due to its relatively low concentrations in house

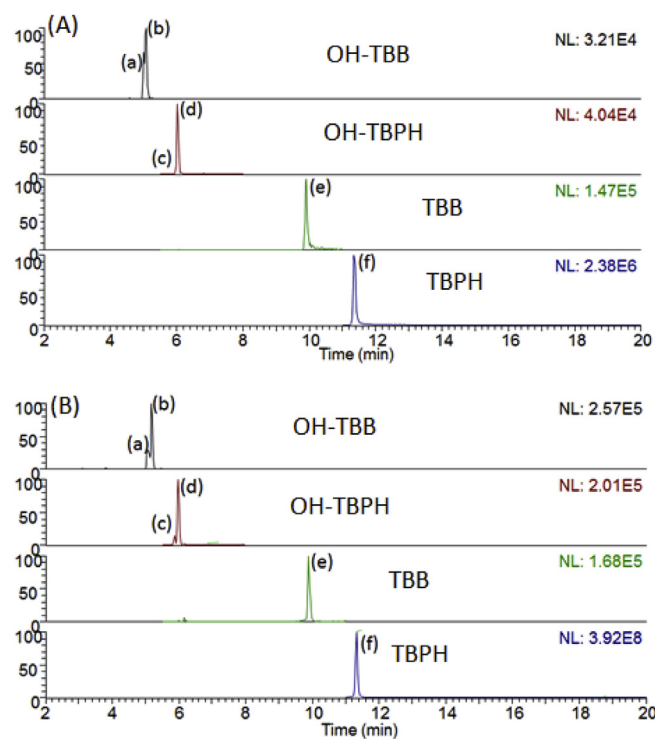


Fig. 3. Typical chromatogram of TBB, TBPH, OH-TBB and OH-TBPH (10 ppm window) in (A) FM-550 and (B) house dust, determined by Q Exactive (SIM) in both APCI (–) and APCI (+).

Table 1

Comparison of ESI and APCI ionization for identification and quantification of OH-TBB, OH-TBPH, TBB and TBPH.

	ESI			IDL ^b	Ion mode	APCI		
	Ion mode	m/z	ions			m/z	ions	IDL
OH-TBB	Negative	484.8789	[M-H] [–]	0.008	Negative	404.9526	[M-H-Br] [–]	0.006
OH-TBPH	Negative	640.9946	[M-H] [–]	0.005 ^c	Negative	640.9946	[M-H] [–]	0.005
TBB	– ^a	–	–	–	Negative	484.8789	[M-Br + O] [–]	0.83
TBPH	Positive	723.9486	[M + NH ₄] ⁺	0.01	Positive	723.9486	[M + NH ₄] ⁺	0.02

^a TBB could not be detected by ESI source.

^b Instrument limit of detection (IDL), µg/L.

^c IDLs of OH-TBPH and TBPH using ESI has been reported previously (Peng et al., 2015).

dust. This conclusion was supported by the similar low concentration of OH-TBB2 in house dust compared to technical products. The three isomers of OH-TBB could not be separated at baseline in both purified standard and dust samples, partly due to the lesser abundance of the first isomer and also due to the decreasing ability to separate OH-TBBs following multiple injections on the HPLC column. Therefore, total concentrations of OH-TBB isomers were quantified based on a single peak. Since OH-TBB could not be detected in full scan mode (Fig. S6), SIM mode was used in this study to detect OH-TBB in dust. This is because total injected ions were limited to a narrow isolation window (2.0 m/z) during analysis by SIM mode, which greatly increased the number of injected ions for targeted chemicals and expanded the dynamic range of the method performance compared to full scan mode.

Relative concentrations of OH-TBB, TBB, OH-TBPH and TBPH in dust were compared to technical products to determine if those mixtures might be sources of isomers in dust. Concentrations of OH-TBBs (geometric mean of 0.21 ng/g, 95% confidence interval (CI), 0.08–0.55 ng/g) in house dust were 2-fold less than those of OH-TBPHs (0.35 ng/g, (95% CI, 0.18–0.69 ng/g) for OH-TBPH2 and 0.04 ng/g (95% CI, 0.02–0.07 ng/g), for OH-TBPH1) (Table 2), which, as discussed above, is consistent with profiles in FM-550 and BZ-54. Although the three peaks of OH-TBB isomers could not be completely resolved or integrated separately, relative intensities of the isomers in dust were similar to intensities observed in BZ-54 (Fig. 2B and Fig. 3B). In BZ-54 the peak abundance of OH-TBB2 was approximately 2-fold less than that of OH-TBB3, which was similar to samples of dust, while the peak abundance of OH-TBB2 was similar to that of OH-TBB3 in FM-550 (Fig. 2A). TBB was detected in all samples of dust with a geometric mean concentration of 922 ng/g (95% CI, 617–1590 ng/g) (Fig. 4A). Concentrations of TBB were comparable to those of TBPH in the same samples of dust (734 ng/g, 95% CI, 430–1250 ng/g), which was similar to another study that detected similar concentrations of TBB and TBPH in house dust (Stapleton et al., 2008). To further evaluate potential emission sources of TBB and TBPH, f_{TBB} was calculated (Equation (1)) to be 0.54 ± 0.16 (Fig. 4B), which was less than in samples of dust from the USA (0.81) (Stapleton et al., 2008), similar to those observed in a previous investigation of TBB and TBPH in samples of air from Chicago (0.545 ± 0.024) (Ma et al., 2012), but greater than those at other locations such as Point Petre, ON, Canada (0.261 ± 0.065) (Ma et al., 2012), indicating the region-specific emission sources of TBB and TBPH. Compared to technical products, the f_{TBB} calculated in this study was similar to those of BZ-54 ($f_{TBB} = 0.61$) but less than those of FM-550 (0.74). BZ-54, FM-550, along with the flame retardant product, DP-45 (100% TBPH), are three potential major sources of TBPH and TBB in the

environment. Results of f_{TBB} and profiles of isomers of OH-TBB indicate that BZ-54 is likely the major source of TBB and TBPH in samples investigated in this study. Additionally, and in accordance with our previous study on TBPH and OH-TBPH (Peng et al., 2015), greater concentrations of OH-TBB and TBB were detected in three samples of dust from a house constructed in 2004 (Fig. 4A), compared to other samples of dust from houses that were constructed more than 20 years ago. This might be due to greater amounts of newer consumer items that adhere to Californian furniture flammability standards (TB117) in the home.

Use of log-linear regression revealed a significant relationship between concentrations of TBB and TBPH ($r^2 = 0.87$, $p < 0.001$), or TBB and OH-TBB ($r^2 = 0.64$, $p < 0.001$) (Fig. 4C). A log-linear relationship between concentrations of OH-TBBs and isomers of OH-TBPH ($r^2 = 0.87$ for OH-TBPH2 and $r^2 = 0.55$ for OH-TBPH1) ($p < 0.01$ for both) was also observed (Fig. 4D). Correlations among concentrations of chemicals along with evidence of similar profiles of chemicals in dust and technical products indicated their common emission sources. However, it should be noted that the ratio of OH-TBB to TBB (P_{OH-TBB}) (Equation (3)) was $0.02\% \pm 0.83$ (Fig. 4B), significantly less than in BZ-54 (1.3%) and FM-550 (0.8%). This phenomenon was also observed for isomers of OH-TBPH in a previous study (Peng et al., 2015). The relatively small contributions of OH-TBB and OH-TBPH in house dust might be due to different physical-chemical properties and environmental fates during application, or mechanical or chemical emissions from products to the environment.

Although the mean concentration of OH-TBB was relatively less than four other target chemicals, the maximum concentration of OH-TBB was relatively great (91 ng/g) which was 3-fold greater than the maximum concentration of total OH-TBPH. In addition, considering the lower Log K_{OW} value of OH-TBB (predicted to be 6.8 using ChemDraw Ultra 8.0) compared to OH-TBPH (predicted to be 9.56 using ChemDraw Ultra 8.0) and TBPH (11.95), the bio-accessibility of OH-TBB would likely be greater than other compounds which indicated that this chemical might pose a greater risk to organisms (Fang and Stapleton, 2014). Two recent studies have reported the presence of TBBA in human urine (Butt et al., 2014; Hoffman et al., 2014), which highlighted the exposure of humans to TBB, and suggested intake of OH-TBB, as concentrations of these compounds are greatly correlated in dust.

3.4. Agonistic potency of OH-TBB and TBB on AR, ER, and PPAR γ

Agonistic interactions with nuclear receptors are important mechanisms of toxicity of phenolic compounds (Matthews et al., 2001; Riu et al., 2011), thus, *in vitro* cellular assays were used to evaluate the potencies of OH-TBB and TBB as agonists of ER, PPAR γ and AR. Potencies of TBB and mixtures of OH-TBB were quantified at concentrations from 8 to 5000 $\mu\text{g/L}$, because concentrations greater than 5000 $\mu\text{g/L}$ exceeded the limit of solubility or caused cytotoxicity.

Neither OH-TBB nor TBB were agonists of the AR, and OH-TBB did not cause any estrogenic response at either concentrations (Fig. S7). However, exposure to 5000 $\mu\text{g/L}$ of mixture of OH-TBB caused a significant estrogenic response (1.74 ± 0.35 fold; $p = 0.04$) compared to solvent control, though the response was less than the response to E2 (1.5 nM) (Fig. 5A). The relative estrogenic potency (ReP) of mixture of OH-TBB was determined to be 4.8×10^{-6} when using the LOEC for calculation (Equation (5)), as described before (Villeneuve et al., 2000). The ReP of mixture of OH-TBB was less than those of nonylphenol (1.25×10^{-5}) and octylphenol (1.9×10^{-5}), but similar to bisphenol A (1.6×10^{-6}), when determined by use of the same MVLN bioassay (Khim et al., 1999). The observed estrogenic potency of OH-TBB is not

Table 2
Concentrations of OH-TBB, TBB, OH-TBPH and TBPH (ng/g) in samples of house dust from Saskatoon, SK, Canada.

	GM ^a	Min	Max	Detected %
TBB	992 (617–1590) ^c	25	38000	100
OH-TBB	0.21 (0.08–0.55)	<0.02	91	91
TBPH ^b	734 (430–1250)	15	22300	100
OH-TBPH1	0.04 (0.02–0.07)	<0.02	7.3	52
OH-TBPH2	0.35 (0.18–0.69)	<0.02	27	91

^a GM indicates geometric mean.

^b Concentrations of TBPH and OH-TBPH in the same dust sample were determined previously (Peng et al., 2015).

^c 95% confidence interval of the concentrations.

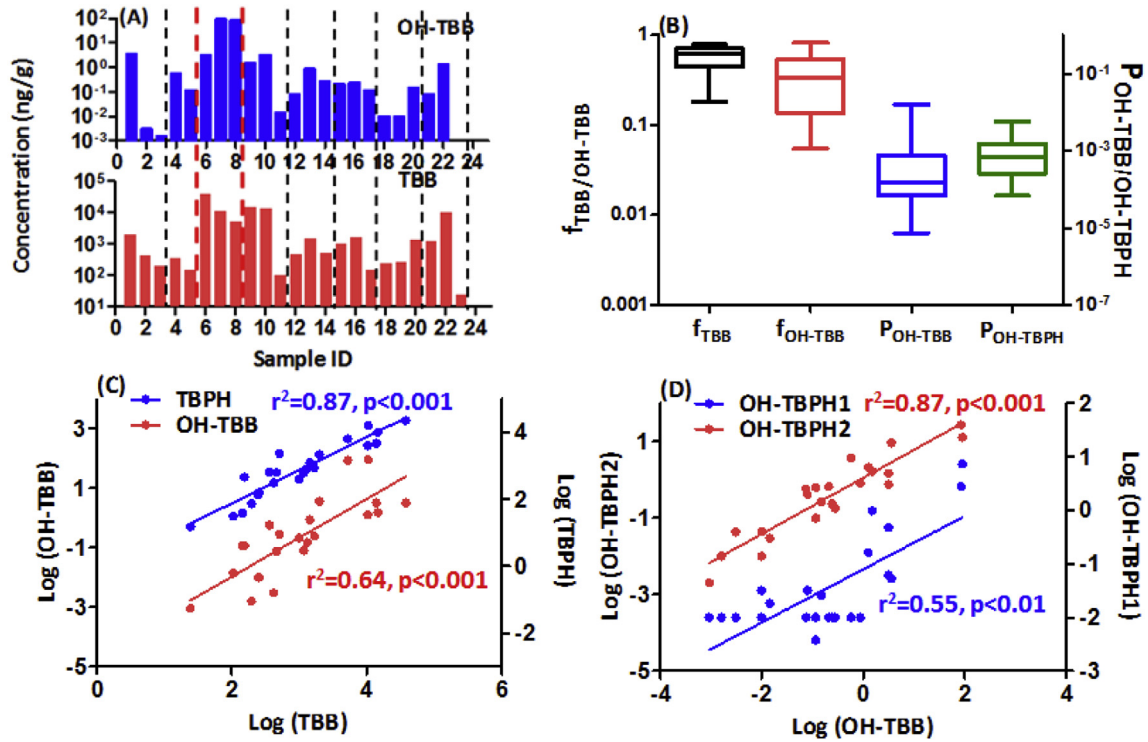


Fig. 4. (A) Concentrations of OH-TBB and TBB in 23 samples of dust from 8 houses in Saskatoon, SK, Canada. Dotted lines separated dust samples among houses. Samples between the two red bold dotted lines, which had greater concentrations of TBB and OH-TBB, were from a house built in 2004. (B) Fraction of TBB to TBPH, fraction of OH-TBB to OH-TBPH, and percentage of OH-TBB to native TBB, and percentage of OH-TBPH to native TBPH in dust samples. (C) Log-linear regression analysis of concentrations of TBB and OH-TBB and TBPH in samples of house dust. (D) Log-linear regression analysis of concentrations of OH-TBB and OH-TBPH in samples of house dust. (For interpretation of the references to colour in this figure legend, the reader is referred to the web version of this article.)

surprising because some phenolic compounds have been reported to exhibit estrogenic activities. For example, parabens and their halogenated disinfectant products have structures that are similar to OH-TBB (Fig. S8), and have estrogenic activities (Watanabe et al., 2013). In addition, the position of the phenol group on the aromatic ring is critical for estrogenic activities. Thus, identification of the exact structures of the three OH-TBB isomers in future studies will be important to understand the estrogenic activities of individual OH-TBB isomers.

Mixture of OH-TBB exhibited relatively strong PPAR γ activity with a clear dose-response relationship, and a significant response was observed even at 40 $\mu\text{g/L}$ (1.77 ± 0.23 fold, $p = 0.005$) (Fig. 5B).

The maximal induced response to mixture of OH-TBB was 10.2 ± 0.72 fold at 5000 $\mu\text{g/L}$, which was even greater than that of rosiglitazone at 20 nM (7.58 ± 0.65 fold). A weak response mediated by PPAR γ was detected for TBB at the highest concentration (5000 $\mu\text{g/L}$). It was previously reported that TBB didn't cause significant effects even at 90 μM (Pillai et al., 2014). The detection of weak potency of TBB as a PPAR γ agonist in the present study might be due to the strong responsiveness of the bioassay (half maximal effective concentration, EC₅₀, was 85.7 nM). The observation of greater potency as a PPAR γ agonist of hydroxylated brominated compounds than their native compounds has been also reported for OH-PBDEs (compared to PBDEs), and TBBPA (compared to

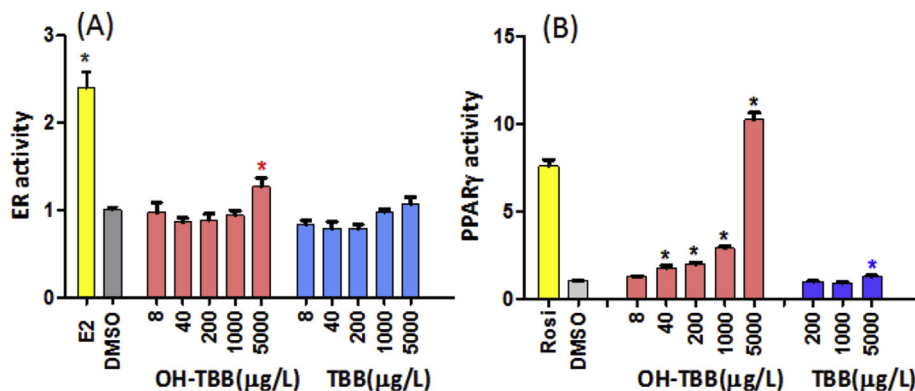


Fig. 5. Estrogenic (A) and PPAR γ (B) potencies of OH-TBB and TBB measured by use of *in vitro* bioassay. Activity is presented as fold-change compared to control (ethanol). Exposure to E2 (1.5 nM) was used as a positive control for an estrogenic response. Exposure to rosiglitazone (20 nM) was used as a positive control for a PPAR γ response. An asterisk (*) indicates a significant response ($p < 0.05$).

bisphenol A) (Fang et al., 2015a; Riu et al., 2011). The crystal structure of the PPAR γ -TBBPA complex showed that the combination of the hydrogen bond of phenolic group and van der Waals interaction of bromine atoms is necessary to maintain the fit of the hydroxylated compounds to the binding pocket of PPAR γ . The ReP of mixture of OH-TBB relative to rosiglitazone was determined to be 0.0006, which was less than that of triphenyltin chloride (TPT) (0.13), but comparable to that of TBBPA (0.002) and triphenyl phosphate (TPP) (0.0002) based on a human embryonic kidney 293 (HEK 293) reporter assay (Fang et al., 2015b).

3.5. Calculation of TEQ_{PPAR γ}

Only TEQs for PPAR γ (TEQ_{PPAR γ}) were calculated for OH-TBB and TBB. Potencies of these two compounds as ER agonists were weak which limited the accuracy of the ReP calculation. Based on compositions of technical products (70% of TBB in BZ-54, and 35% in FM-550) (Ma et al., 2012), concentrations of TEQ_{PPAR γ} for TBB were 7.12 and 3.56 ng/g in BZ-54 and FM-550 respectively. These concentrations of TEQ were comparable to those of mixture of OH-TBB (5.78 and 1.78 ng/g in BZ-54 and FM-550). The concentration of TEQ_{PPAR γ} of OH-TBBs in FM-550 was approximately 10-fold less than that of TPP, which was 22.9 ng/g, based on concentrations (10–20%) in FM-550 (Fang et al., 2015b; Pillai et al., 2014). This is consistent with previous results that TPP was a major contributor to PPAR γ agonist potency in FM-550 (Pillai et al., 2014). Despite the relatively large contribution of OH-TBBs to PPAR γ agonist potency in technical products, the concentration of TEQ_{PPAR γ} of OH-TBBs in house dust (0.13 pg/g) was 100-fold less than that of TBB (10.1 pg/g). This result was primarily due to the small concentration of OH-TBBs in house dust. The lesser contributions of OH-TBBs in samples of house dust, compared to technical products, indicated preferential emission of OH-TBBs to other environmental matrices, and future studies are warranted to clarify the potential exposure of humans to TEQ_{PPAR γ} from OH-TBBs via other routes of exposure. In addition, because of its lesser K_{OW} values, OH-TBBs might be easily absorbed by humans and wildlife.

In conclusion, novel OH-TBB isomers were identified in the technical products, FM-550 and BZ-54 and samples of house dust. The greater estrogenic and PPAR γ potencies of OH-TBB than native TBB, together with their low K_{OW} values and occurrence in house dust indicated their potential risk to humans. A new LC-APCI-Q Exactive method was developed, provided a chance for convenient and simultaneous determination of OH-TBB, TBB, OH-TBPH and TBPH in house dust samples.

Acknowledgement

The authors would like to thank Mingliang Fang of the Heather Stapleton Research Group, Duke University, Nicholas School of the Environment for providing Firemaster[®] technical products. D.M.V.S was supported by the Vanier Canada Graduate Scholarship. J.P.G. was supported by the Canada Research Chair program, a Visiting Distinguished Professorship in the Department of Biology and Chemistry and State Key Laboratory in Marine Pollution, City University of Hong Kong, the 2012 “High Level Foreign Experts” (GDW20223200120) program funded by the State Administration of Foreign Experts Affairs, the P. R. China to Nanjing University, and the Einstein Professor Program of the Chinese Academy of Sciences. The research was supported by a Discovery Grant from the Natural Sciences and Engineering Research Council of Canada (Project # 326415-07) and a grant from the Western Economic Diversification Canada (Project # 6578 and 6807). The authors wish to acknowledge the support of an instrumentation grant from Western Economic Diversification (WED) (000012711).

Appendix A. Supplementary data

Supplementary data related to this article can be found at <http://dx.doi.org/10.1016/j.envpol.2017.04.094>.

References

- Alaee, M., Wenning, R.J., 2002. The significance of brominated flame retardants in the environment: current understanding, issues and challenges. *Chemosphere* 46 (5), 579–582.
- Allen, J.G., McClean, M.D., Stapleton, H.M., Webster, T.F., 2008. Critical factors in assessing exposure to PBDEs via house dust. *Environ. Int.* 34 (8), 1085–1091.
- Alm, H., Scholz, B., Kultima, K., Nilsson, A., Andren, P.E., Savitski, M.M., et al., 2010. In vitro neurotoxicity of PBDE-99: immediate and concentration-dependent effects on protein expression in cerebral cortex cells. *J. Proteome Res.* 9 (3), 1226–1235.
- Bearr, J.S., Stapleton, H.M., Mitchelmore, C.L., 2010. Accumulation and DNA damage in Fathead Minnow (*Pimephales Promelas*) exposed to 2 brominated flame-retardant mixtures, Firemaster (R) 550 and Firemaster (R) BZ-54. *Environ. Toxicol. Chem.* 29 (3), 722–729.
- Birnbaum, L.S., Staskal, D.F., 2004. Brominated flame retardants: cause for concern? *Environ. Health Perspect.* 112 (1), 9–17.
- Butt, C.M., Congleton, J., Hoffman, K., Fang, M.L., Stapleton, H.M., 2014. Metabolites of organophosphate flame retardants and 2-ethylhexyl tetrabromobenzoate in urine from paired mothers and toddlers. *Environ. Sci. Technol.* 48 (17), 10432–10438.
- Chang, H., Wan, Y., Naile, J., Zhang, X.W., Wiseman, S., Hecker, M., et al., 2010. Simultaneous quantification of multiple classes of phenolic compounds in blood plasma by liquid chromatography-electrospray tandem mass spectrometry. *J. Chromatogr. A* 1217 (4), 506–513.
- Chen, D., Hale, R.C., 2010. A global review of polybrominated diphenyl ether flame retardant contamination in birds. *Environ. Int.* 36 (7), 800–811.
- Chen, D., Letcher, R.J., Martin, P., 2012. Flame retardants in eggs of American kestrels and European starlings from southern Lake Ontario region (North America). *J. Environ. Monit.* 14 (11), 2870–2876.
- Fang, M.L., Stapleton, H.M., 2014. Evaluating the bioaccessibility of flame retardants in house dust using an in vitro tenax bead-assisted sorptive physiologically based method. *Environ. Sci. Technol.* 48 (22), 13323–13330.
- Fang, M.L., Webster, T.F., Ferguson, P.L., Stapleton, H.M., 2015a. Characterizing the peroxisome proliferator-activated receptor (PPAR gamma) ligand binding potential of several major flame retardants, their metabolites, and chemical mixtures in house dust. *Environ. Health Perspect.* 123 (2), 166–172.
- Fang, M.L., Webster, T.F., Stapleton, H.M., 2015b. Activation of human peroxisome proliferator-activated nuclear receptors (PPAR gamma 1) by semi-volatile compounds (SVOCs) and chemical mixtures in indoor dust. *Environ. Sci. Technol.* 49 (16), 10057–10064.
- Grun, F., Blumberg, B., 2007. Perturbed nuclear receptor signaling by environmental obesogens as emerging factors in the obesity crisis. *Rev. Endocr. Metab. Disord.* 8 (2), 161–171.
- Hakk, H., Letcher, R.J., 2003. Metabolism in the toxicokinetics and fate of brominated flame retardants—a review. *Environ. Int.* 29 (6), 801–828.
- Hoffman, K., Fang, M.L., Horman, B., Patisaul, H.B., Garantzios, S., Birnbaum, L.S., et al., 2014. Urinary tetrabromobenzoic acid (TBBA) as a biomarker of exposure to the flame retardant mixture Firemaster (R) 550. *Environ. Health Perspect.* 122 (9), 963–969.
- Jenkins, S., Raghuraman, N., Eltoum, I., Carpenter, M., Russo, J., Lamartiniere, C.A., 2009. Oral exposure to bisphenol A increases dimethylbenzanthracene-induced mammary cancer in rats. *Environ. Health Perspect.* 117 (6), 910–915.
- Kato, Y., Okada, S., Atobe, K., Endo, T., Matsubara, F., Oguma, T., et al., 2009. Simultaneous determination by APCI-LC/MS/MS of hydroxylated and methoxylated polybrominated diphenyl ethers found in marine biota. *Anal. Chem.* 81 (14), 5942–5948.
- Khim, J.S., Villeneuve, D.L., Kannan, K., Koh, C.H., Giesy, J.P., 1999. Characterization and distribution of trace organic contaminants in sediment from Masan Bay, Korea. 2. In vitro gene expression assays. *Environ. Sci. Technol.* 33 (23), 4206–4211.
- Klopčič, I., Skledar, G., Masić, L.P., Dolenc, M.S., 2016. Comparison of in vitro hormone activities of novel flame retardants TBB, TBPH and their metabolites TBBA and TBMEPH using reporter gene assays. *Chemosphere* 160, 244–251.
- Klosterhaus, S.L., Stapleton, H.M., La Guardia, M.J., Greig, D.J., 2012. Brominated and chlorinated flame retardants in San Francisco Bay sediments and wildlife. *Environ. Int.* 47, 56–65.
- Kohler, M., Zennegg, M., Bogdal, C., Gerecke, A.C., Schmid, P., Heeb, N.V., et al., 2008. Temporal trends, congener patterns, and sources of Octa-, Nona-, and decabromodiphenyl ethers (PBDE) and hexabromocyclododecanes (HBCD) in Swiss lake sediments. *Environ. Sci. Technol.* 42 (17), 6378–6384.
- Lake, I.R., Foxall, C.D., Fernandes, A., Lewis, M., Rose, M., White, O., et al., 2011. Effects of river flooding on polybrominated diphenyl ether (PBDE) levels in cows' milk, soil, and grass. *Environ. Sci. Technol.* 45 (11), 5017–5024.
- Leung, A.O., Luksemburg, W.J., Wong, A.S., Wong, M.H., 2007. Spatial distribution of polybrominated diphenyl ethers and polychlorinated dibenzo-p-dioxins and dibenzofurans in soil and combusted residue at Guiyu, an electronic waste recycling site in southeast China. *Environ. Sci. Technol.* 41 (8), 2730–2737.

- Liu, H.H., Hu, Y.J., Luo, P., Bao, L.J., Qiu, J.W., Leung, K.M.Y., et al., 2014. Occurrence of halogenated flame retardants in sediment off an urbanized coastal zone: association with urbanization and industrialization. *Environ. Sci. Technol.* 48 (15), 8465–8473.
- Loukou, Z., Zotou, A., 2003. Determination of biogenic amines as dansyl derivatives in alcoholic beverages by high-performance liquid chromatography with fluorimetric detection and characterization of the dansylated amines by liquid chromatography-atmospheric pressure chemical ionization mass spectrometry. *J. Chromatogr. A* 996 (1–2), 103–113.
- Ma, Y.N., Salamova, A., Venier, M., Hites, R.A., 2013. Has the phase-out of PBDEs affected their atmospheric levels? trends of PBDEs and their replacements in the Great Lakes atmosphere. *Environ. Sci. Technol.* 47 (20), 11457–11464.
- Ma, Y.N., Venier, M., Hites, R.A., 2012. 2-Ethylhexyl tetrabromobenzoate and bis(2-ethylhexyl) tetrabromophthalate flame retardants in the Great Lakes atmosphere. *Environ. Sci. Technol.* 46 (1), 204–208.
- Matthews, J.B., Twomey, K., Zacharewski, T.R., 2001. In vitro and in vivo interactions of bisphenol A and its metabolite, bisphenol A glucuronide, with estrogen receptors alpha and beta. *Chem. Res. Toxicol.* 14 (2), 149–157.
- Mercado-Feliciano, M., Bigsby, R.M., 2008. Hydroxylated metabolites of the polybrominated diphenyl ether mixture DE-71 are weak estrogen receptor-alpha ligands. *Environ. Health Perspect.* 116 (10), 1315–1321.
- Moller, A., Xie, Z.Y., Cai, M.H., Zhong, G.C., Huang, P., Cai, M.G., et al., 2011. Polybrominated diphenyl ethers vs alternate brominated flame retardants and dechloranes from East Asia to the Arctic. *Environ. Sci. Technol.* 45 (16), 6793–6799.
- Muirhead, E.K., Skillman, D., Hook, S.E., Schultz, I.R., 2006. Oral exposure of PBDE-47 in fish: toxicokinetics and reproductive effects in Japanese medaka (*Oryzias latipes*) and fathead minnows (*Pimephales promelas*). *Environ. Sci. Technol.* 40 (2), 523–528.
- Newbold, R.R., Jefferson, W.N., Padilla-Banks, E., 2009. Prenatal exposure to bisphenol A at environmentally relevant doses adversely affects the murine female reproductive tract later in life. *Environ. Health Perspect.* 117 (6), 879–885.
- Peng, H., Hu, K.J., Zhao, F.R., Hu, J.Y., 2013. Derivatization method for sensitive determination of fluorotelomer alcohols in sediment by liquid chromatography-electrospray tandem mass spectrometry. *J. Chromatogr. A* 1288, 48–53.
- Peng, H., Saunders, D.M.V., Sun, J.X., Garry, C., Wiseman, S., Jones, P.D., et al., 2015. Detection, identification, and quantification of hydroxylated bis(2-ethylhexyl)-tetrabromophthalate isomers in house dust. *Environ. Sci. Technol.* 49, 2999–3006.
- Peng, H., Saunders, D.M.V., Sun, J.X., Jones, P.D., Wong, C.K.C., Liu, H.L., et al., 2016. Mutagenic azo dyes, rather than flame retardants, are the predominant brominated compounds in house dust. *Environ. Sci. Technol.* 50 (23), 12669–12677.
- Pillai, H.K., Fang, M.L., Beglov, D., Kozakov, D., Vajda, S., Stapleton, H.M., et al., 2014. Ligand binding and activation of PPAR gamma by Firemaster (R) 550: effects on adipogenesis and osteogenesis in vitro. *Environ. Health Perspect.* 122 (11), 1225–1232.
- Riu, A., Grimaldi, M., le Maire, A., Bey, G., Phillips, K., Boulahtouf, A., et al., 2011. Peroxisome proliferator-activated receptor gamma is a target for halogenated analogs of bisphenol A. *Environ. Health Perspect.* 119 (9), 1227–1232.
- Saunders, D.M.V., Higley, E.B., Hecker, M., Mankidy, R., Giesy, J.P., 2013. In vitro endocrine disruption and TCDD-like effects of three novel brominated flame retardants: TBPH, TBB, & TBCO. *Toxicol. Lett.* 223 (2), 252–259.
- Skledar, D.G., Tomasic, T., Carino, A., Distrutti, E., Fiorucci, S., Masic, L.P., 2016. New brominated flame retardants and their metabolites as activators of the pregnane X receptor. *Toxicol. Lett.* 259, 116–123.
- Springer, C., Dere, E., Hall, S.J., McDonnell, E.V., Roberts, S.C., Butt, C.M., et al., 2012. Rodent thyroid, liver, and fetal testis toxicity of the monoester metabolite of bis-(2-ethylhexyl) tetrabromophthalate (TBPH), a novel brominated flame retardant present in indoor dust. *Environ. Health Perspect.* 120 (12), 1711–1719.
- Stapleton, H.M., Allen, J.G., Kelly, S.M., Konstantinov, A., Klosterhaus, S., Watkins, D., et al., 2008. Alternate and new brominated flame retardants detected in US house dust. *Environ. Sci. Technol.* 42 (18), 6910–6916.
- Stapleton, H.M., Misenheimer, J., Hoffman, K., Webster, T.F., 2014. Flame retardant associations between children's handwipes and house dust. *Chemosphere* 116, 54–60.
- Szarka, S., Nguyen, V., Prokai, L., Prokai-Tatrai, K., 2013. Separation of dansylated 17 beta-estradiol, 17 alpha-estradiol, and estrone on a single HPLC column for simultaneous quantitation by LC-MS/MS. *Anal. Bioanal. Chem.* 405 (10), 3399–3406.
- Villeneuve, D.L., Blankenship, A.L., Giesy, J.P., 2000. Derivation and application of relative potency estimates based on in vitro bioassay results. *Environ. Toxicol. Chem.* 19 (11), 2835–2843.
- Vorkamp, K., Bossi, R., Riget, F.F., Skov, H., Sonne, C., Dietz, R., 2015. Novel brominated flame retardants and dechlorane plus in Greenland air and biota. *Environ. Pollut.* 196, 284–291.
- Wan, Y., Hu, J.Y., Zhang, K., An, L.H., 2008. Trophodynamics of polybrominated diphenyl ethers in the marine food web of Bohai Bay, North China. *Environ. Sci. Technol.* 42 (4), 1078–1083.
- Watanabe, Y., Kojima, H., Takeuchi, S., Uramaru, N., Ohta, S., Kitamura, S., 2013. Comparative study on transcriptional activity of 17 parabens mediated by estrogen receptor alpha and beta and androgen receptor. *Food Chem. Toxicol.* 57, 227–234.
- Wolkers, H., Van Bavel, B., Derocher, A.E., Wiig, O., Kovacs, K.M., Lydersen, C., et al., 2004. Congener-specific accumulation and food chain transfer of polybrominated diphenyl ethers in two Arctic food chains. *Environ. Sci. Technol.* 38 (6), 1667–1674.
- Xie, Z.Y., Moller, A., Ahrens, L., Sturm, R., Ebinghaus, R., 2011. Brominated flame retardants in seawater and atmosphere of the Atlantic and the Southern Ocean. *Environ. Sci. Technol.* 45 (5), 1820–1826.
- Zhou, S.N., Buchar, A., Siddique, S., Takser, L., Abdelouahab, N., Zhu, J.P., 2014. Measurements of selected brominated flame retardants in nursing women: implications for human exposure. *Environ. Sci. Technol.* 48 (15), 8873–8880.
- Zhou, S.N., Reiner, E.J., Marvin, C., Helm, P., Riddell, N., Dorman, F., et al., 2010. Development of liquid chromatography atmospheric pressure chemical ionization tandem mass spectrometry for analysis of halogenated flame retardants in wastewater. *Anal. Bioanal. Chem.* 396 (3), 1311–1320.
- Zhou, T., Ross, D.G., DeVito, M.J., Crofton, K.M., 2001. Effects of short-term in vivo exposure to polybrominated diphenyl ethers on thyroid hormones and hepatic enzyme activities in weanling rats. *Toxicol. Sci.* 61 (1), 76–82.

Supplementary Material

Title: Hydroxylated 2-Ethylhexyl Tetrabromobenzoate Isomers in House Dust and Their Agonistic Activity with Several Nuclear Receptors

Authors: Hui Peng^a, Jianxian Sun*^a, David M.V. Saunders^a, Garry Codling^a, Steve Wiseman^a, Paul D. Jones^{a,b} and John. P. Giesy^{a,c,d,e,f,g}

^a Toxicology Centre, University of Saskatchewan, 44 Campus Drive, Saskatoon, SK, Canada, S7N 5B3

^b School of Environment and Sustainability, 117 Science Place, Saskatoon, SK, Canada, S7N 5C8

^c Department of Veterinary Biomedical Sciences, University of Saskatchewan, Saskatoon, SK, Canada S7N 5B3

^d Zoology Department, Center for Integrative Toxicology, Michigan State University, East Lansing, MI, USA

^e Department of Biology and Chemistry, City University of Hong Kong, Kowloon, Hong Kong Special Administrative Region, Peoples republic of China

^f School of Biological Sciences, University of Hong Kong, Hong Kong Special Administrative Region, Peoples republic of China

^g State Key Laboratory of Pollution Control and Resource Reuse, School of the Environment, Nanjing University, Nanjing, People's Republic of China

1. Chemicals and reagents

Standards of TBPH (purity, 98.1%) and TBB (purity, >98%) were purchased from AccuStandard (New Haven, CT, USA), and their surrogate standard d_{34} , $^{13}\text{C}_6$ -TBPH (purity, >98%) and d_{17} , $^{13}\text{C}_6$ -TBB (purity, >98%) were purchased from Wellington Laboratories Inc. (Guelph, Ontario, Canada). Rosiglitazone was from Sigma-Aldrich (St. Louis, MO). BZ-54 and FM-550 technical products were gifts from the Heather Stapleton Research Group at Duke University, Nicholas School of the Environment (Durham, NC, USA). OH-TBB were purified from the BZ-54 technical mixture by use of HPLC, and the impurity of native TBB and TBPH were <0.9% and 0.3%. Florisil (6cc, 1 g, 30 μm) solid-phase extraction (SPE) cartridges were purchased from Waters (Milford, MA, USA). Ammonia solution (~28-30%) was purchased from Alfa Aesar Chemical Industries (Ward Hill, MA, USA). Dichloromethane (DCM), methanol, and acetone were all “omni-Solv[®]” grade and were purchased from EMD Chemicals (Gibbstown, NJ, USA). Human PPAR γ reporter assay kit was purchased from Cayman Chemical (Ann Arbor, MI, USA). A cell line derived from human breast cancer cells that have been stably transfected with an estrogen receptor controlled luciferase reporter gene construct (called MVLN) were cultured in Dulbecco’s Modified Eagle Medium (DMEM) with Hams F-12 nutrient mixture (Sigma D-2906; St. Louis, MO, USA) supplemented with 10% defined fetal bovine serum (FBS) (Hyclone, Logan, UT, USA), 27.3 I.U. insulin (Sigma I-1882)/L, and 1.0 mM sodium pyruvate (Sigma, Mississauga, ON, Canada). Dextran-charcoal treated fetal bovine serum (DCC-FBS) used for exposure media was purchased from Hyclone (Logan, UT, USA). All the media were filtered through a 0.22 μm bottle top filter (Corning, Oneonta, NY, USA) to avoid microbial contamination.

2. Purification of OH-TBB by HPLC fractionation

HPLC fractionation was used to isolate OH-TBB from technical product BZ-54 which contained only TBB and TBPH compared to FM-550. Fractions were collected at 2-min interval from 0 min to 120 min, and then OH-TBB in each fraction was quantified by use of UHPLC-Q Exactive after 10,000-fold dilution with a mixture of methanol and acetone (v/v, 1:1). Fractions which contained OH-TBB were collected and combined, and then evaporated. Fractionation was conducted by use of a Betasil C18 column (5 μ m; 22.1 mm \times 150 mm; Thermo Fisher Scientific) which was maintained at 30 °C. The flow rate and the injection volume were 6 mL/min and 100 μ L, respectively. Mixture of methanol and ultrapure water (v/v, 8:2) containing 0.1% NH₄OH (v/v) was used as mobile phase. The purified OH-TBB (1 mg/L) was also characterized using UHPLC-Q Exactive with full scan range from m/z 200-2000. The intensity of OH-TBB was 100-folds higher than TBB, indicated the relatively high purity of the OH-TBB standard (Fig. S3).

3. Sample pretreatment

Approximately 0.1 g, dry mass (dw) of dust was transferred to a 15 ml centrifuge tube and 20 μ l of 1 mg/L mass-labeled internal standard d_{34} , ¹³C₆-TBPH and d_{17} , ¹³C₆-TBB, and 5 ml of methanol were added to each sample for extraction. Samples were shaken vigorously (Heidolph® Multi Reax Vibrating Shaker, Brinkmann®) for 30 minutes followed by sonication for an additional 30 min, and the methanol extract was separated by centrifugation at 1669 \times g for 10 min and transferred to a new tube. The extraction was repeated with 5 mL DCM. The methanol and DCM extracts were combined and blown to dryness under a gentle stream of nitrogen. Extracts were dissolved in 500 μ l of DCM and loaded onto Florisil cartridges, which had been sequentially conditioned by use of 6 mL of acetone and DCM. TBB and TBPH was eluted from the Florisil cartridges by use of 5 mL DCM. Following a washing rinse with 4 mL of acetone, OH-TBB and OH-TBPH isomers were eluted to a new tube by use of 5 mL mixture

of methanol:DCM (v/v, 1:1). Final extracts were blown to dryness under a gentle stream of nitrogen and reconstituted with 200 μ l of acetone for analysis.

Matrix effects for dusts were evaluated by spiking standards after sample preparation. The matrix effects were calculated according to the following equation.

$$\text{Matrix} = \frac{\text{Conc}_{\text{act}} - \text{Conc}_{\text{std}}}{\text{Conc}_{\text{std}}}$$

Where matrix indicates matrix effects, Conc_{act} indicates the concentrations of compounds detected in spiked samples, Conc_{std} indicated the concentrations of standards spiked into samples.

4. Instrumental analysis

Aliquots of extracts were analyzed by use of a Q Exactive mass spectrometer equipped with a Dionex™ UltiMate™ 3000 UHPLC system (Thermo Fisher Scientific). Separation was achieved by use of a Betasil C18 column (5 μ m; 2.1 mm \times 100 mm; Thermo Fisher Scientific) with an injection volume of 5 μ l. Ultrapure water (A) and methanol containing 0.1% NH_4OH (v/v) (B) were used as mobile phases. Initially 20% of B was increased to 80% in 3 min, then increased to 100% at 8 min and held static for 19.5 min, followed by a decrease to initial conditions of 20% B and held for 2 min to allow for equilibration. The flow rate was 0.25 mL/min. Temperatures of the column and sample chamber were maintained at 30 $^\circ\text{C}$ and 10 $^\circ\text{C}$, respectively. Data were acquired by use of one full scan mode, followed by two selected ion monitoring (SIM) with an APCI ionization source. Full scan mode was used to record all the MS^1 information for future retrospective data analysis, but SIM mode was used to monitor the four target compounds to expand dynamic range. Briefly, MS scans (200-2000 m/z) were recorded at resolution $R=70,000$ (at m/z 200) with a maximum of 3×10^6 ions collected within 100 ms, based on the predictive automated gain control. SIM scans were recorded at a resolution

of $R=70,000$ (at m/z 200) with maximum of 5×10^4 ions collected within 80 ms, based on the predictive automated gain control, with isolation width set at 2.0 m/z . For MS^2 identification, selected ions were fragmented in the collision cell by use of higher-energy collisional dissociation (HCD). MS^2 scans with a target value of 1×10^5 ions were collected with a maximum fill time of 120 ms and $R=35,000$ (at m/z 200). The applied general mass spectrometric settings for APCI source were as follows: discharge current, 10 μA ; capillary temperature, 225 $^{\circ}C$; sheath gas, 20 L/h; auxiliary gas, 5 L/h; probe heater temperature, 350 $^{\circ}C$.

5. Cell assay

MVLN cells were used to test estrogenicity. Culture medium for MVLN cells was Dulbecco's Modified Eagle Medium (DMEM)/F12 nutrient mixture (Sigma; St. Louis, MO) supplemented with 10% fetal bovine serum (FBS) (Hyclone, Logan, UT), 1 mg/L insulin (Sigma), and 1 mM sodium pyruvate (Sigma). FBS was replaced with dextran-coated charcoal fetal bovine serum (DCC-FBS, Hyclone) in exposure media. Cells were incubated at 37 $^{\circ}C$, in a 5% humidified CO_2 incubator. For the assay, MVLN cells were diluted in exposure medium to a concentration of approximately 7.5×10^4 cells/mL, and 125 μL was seeded into a 96-well luminometer plate (Perkin-Elmer, Woodbridge, ON, Canada). After overnight incubation, cells were exposed to serial concentrations of chemicals or positive control (1.5 nM E2). After 48 h exposure, activity of luciferase was detected by measurement of light produced by use of the SteadyLitePlus Kit (PerkinElmer, MA, USA) according to the manufacturer's protocols. Briefly, cells were washed with phosphate buffered saline (PBS) at room temperature, and then 75 μL PBS supplemented with Ca^{2+} and Mg^{2+} and 75 μL Luc-lite reagent were added to each well. After incubating for 15 min at room temperature, luminescence was read by use of a POLARStar OPTIMA microplate reader (BMG Labtech, Offenburg, Germany).

PPAR γ agonistic activity was tested using human PPAR γ reporter assay kit (Cayman Chemical, Ann Arbor, MI, USA), according to the manufacturer's instructions. In brief, as for agonistic activity test, positive control (rosiglitazone, 20 nM) or tested compounds were mixed with culture media. 100 μ l of the mixed media and 100 μ l of the reporter cell line suspension was mixed and added to a 96-well plate. After 24 hours of incubation, the culture media was removed and 100 μ L of luciferase detection reagent was added. After 15 min incubation, the luciferase luminescence was quantified by microplate reader.

The androgenicity of TBB and OH-TBB were tested in MDA cells (ATCC, Manassas, VA, USA). MDA cells were maintained in L15 media (Sigma) supplemented with 10% FBS (Sigma) at 37 °C without CO₂. FBS was replaced with 5% DCC-FBS (Hyclone) in exposure media. MDA cells were diluted in exposure medium to 1.6×10^5 cells/mL, and 125 μ L was seeded into a 96-well luminometer plate (Perkin-Elmer). After overnight incubation, cells were exposed to serial concentrations of chemicals or positive control (dihydrotestosterone (DHT), 1.0 μ M). Exposure time was 24 h for MDA cells, and activity of luciferase was detected by use of the SteadylitePlus Kit (PerkinElmer).

For all the cell assays, TBB and OH-TBB were diluted in 5-fold serial in 100% ethanol and tested in four replicates in at least two independent experiments. The starting exposure concentration of TBB and OH-TBB was 5000 μ g/L (~10 μ M), since higher concentrations showed cytotoxicity or limited solubility in medium. The final concentration of ethanol in all exposure was 0.1%. Control experiments demonstrated that this concentration of ethanol did not affect cell viability. Negative control (media alone), solvent control (EtOH) and positive control was included in each assay.

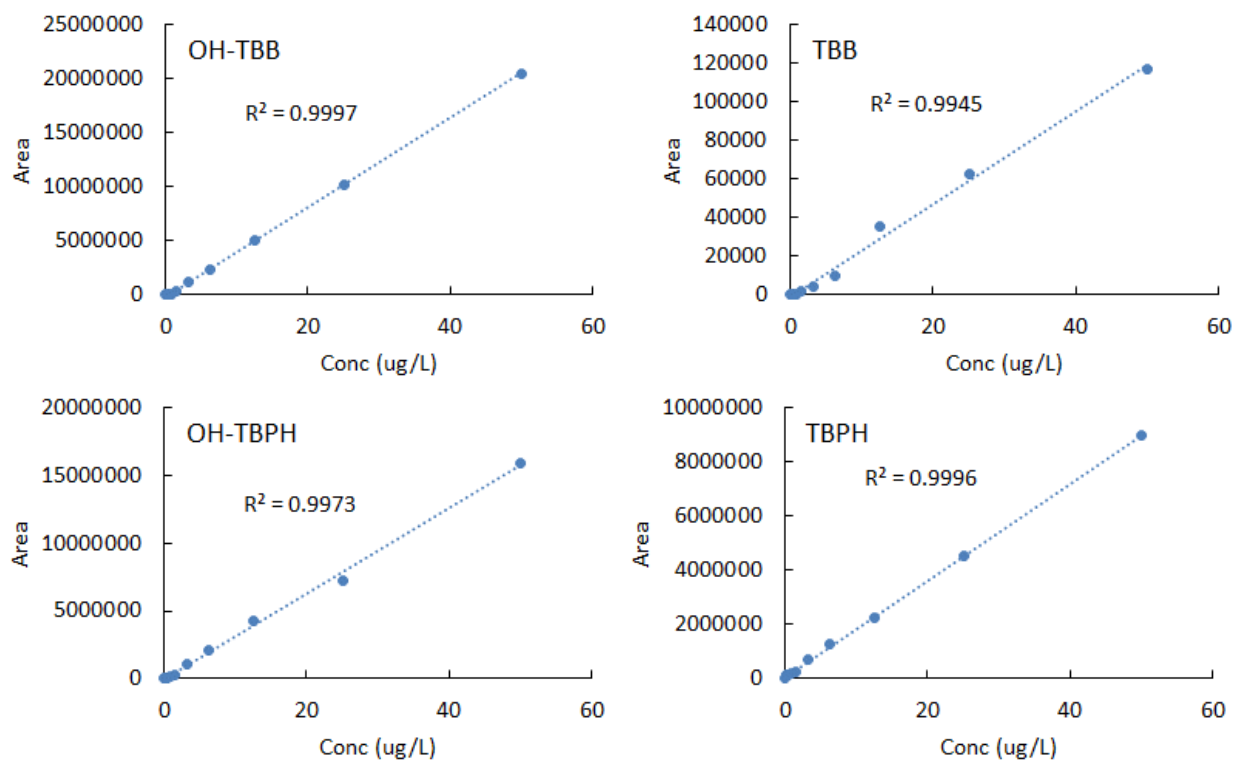


Fig. S1. Calibration curves of OH-TBB, TBB, OH-TBPH and TBPH.

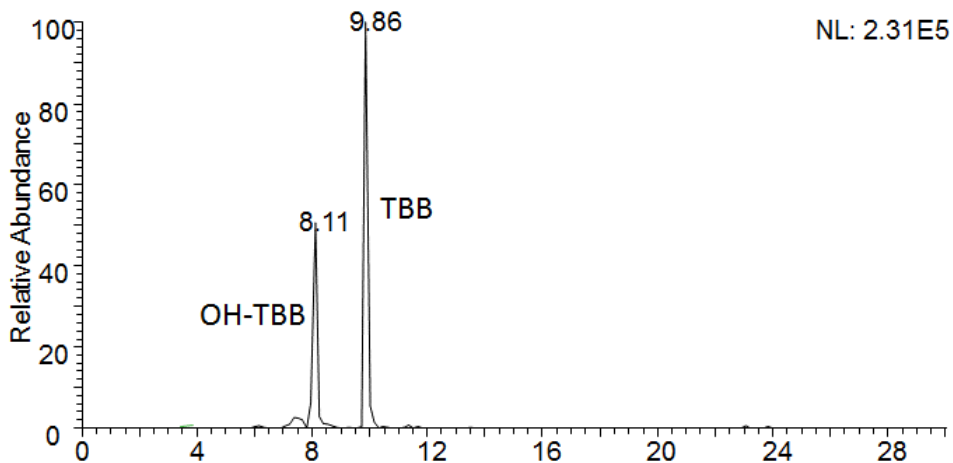


Fig. S2. Chromatogram of isomers of OH-TBB (10 ppm window) in APCI (-) using pure methanol as mobile phase.

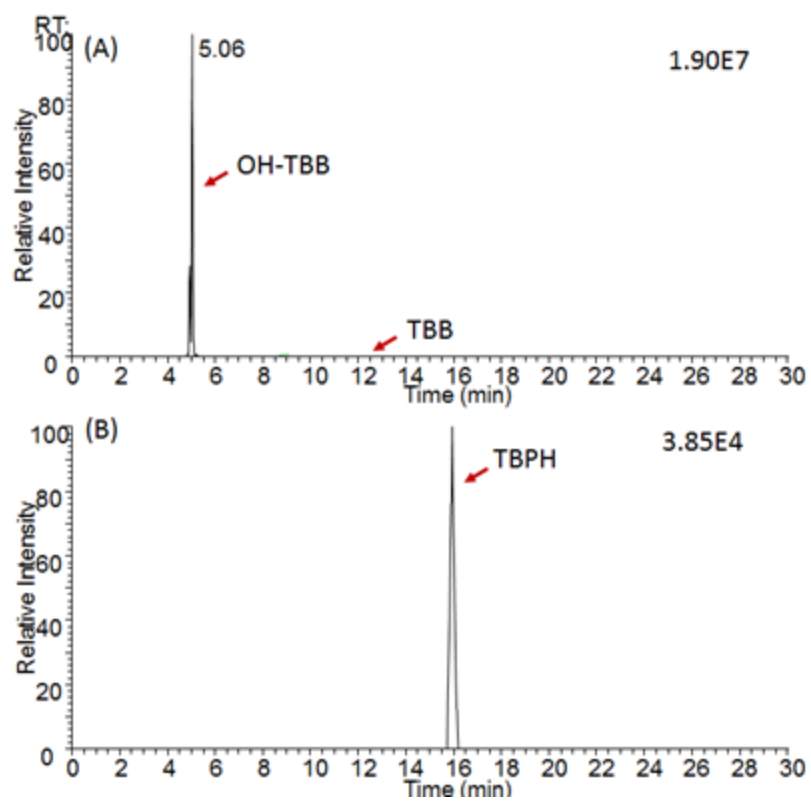


Fig. S3. UPLC-Q Exactive analysis of purified OH-TBB standards. TBB was not detected in the purified standard. The impurities of TBB and TBPH were calculated to be <0.9% and 0.3% respectively.

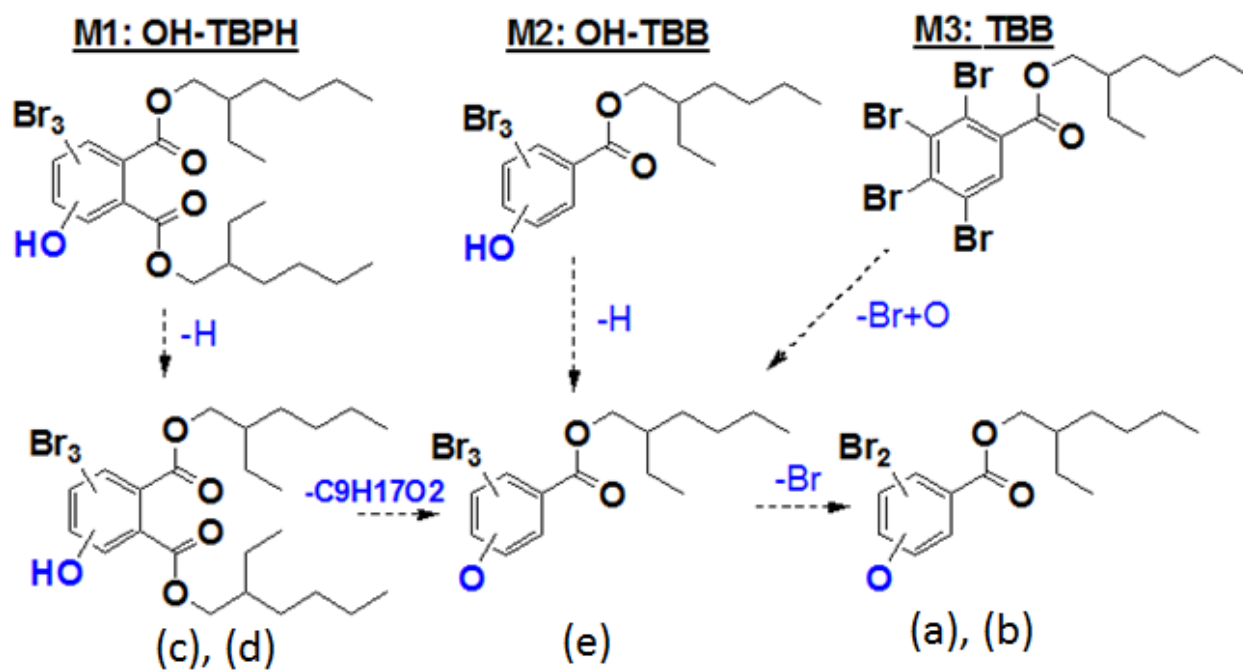


Fig. S4. Ionization routes of OH-TBPH, OH-TBB and TBB in APCI (-) source. (a) OH-TBB2; (b) OH-TBB3; (c) OH-TBPH1; (d) OH-TBPH2; (e) TBB; (f) TBPH.

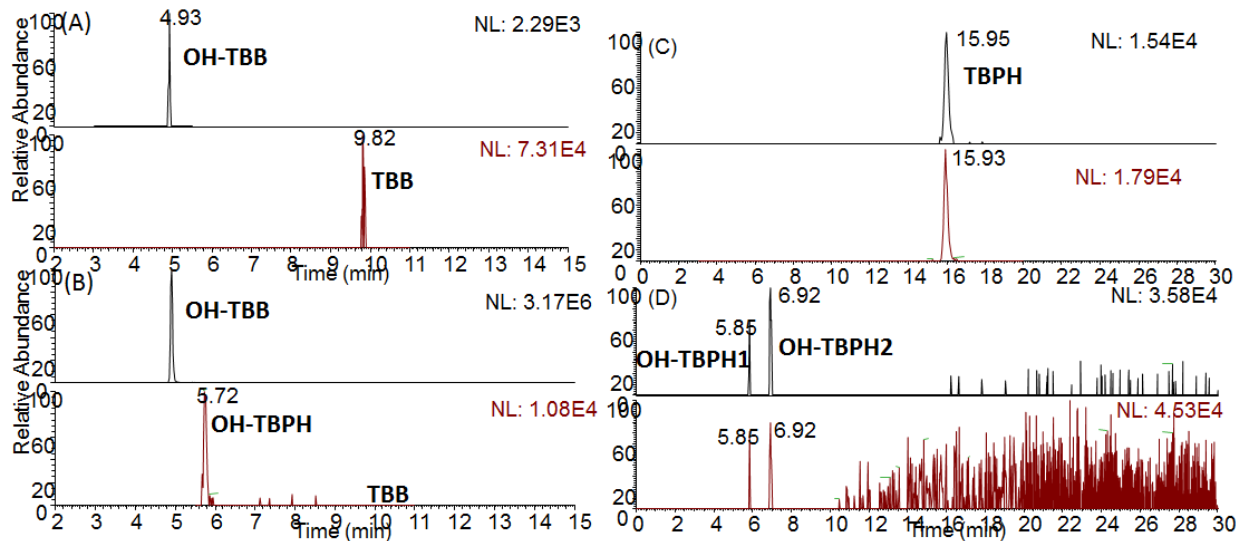


Fig. S5. (A) TBB and TBPH (C) were eluted in the first fraction from Florisil cartridges using DCM; (B) OH-TBB isomers and (D) OH-TBPH isomers were eluted in the third fraction from Florisil cartridges using a mixture of methanol:DCM (v/v, 1:1). All the compounds were quantified using the ions from Table 1 except for OH-TBPH peak from (B) is the fragment ion which exhibited the same m/z with OH-TBB.

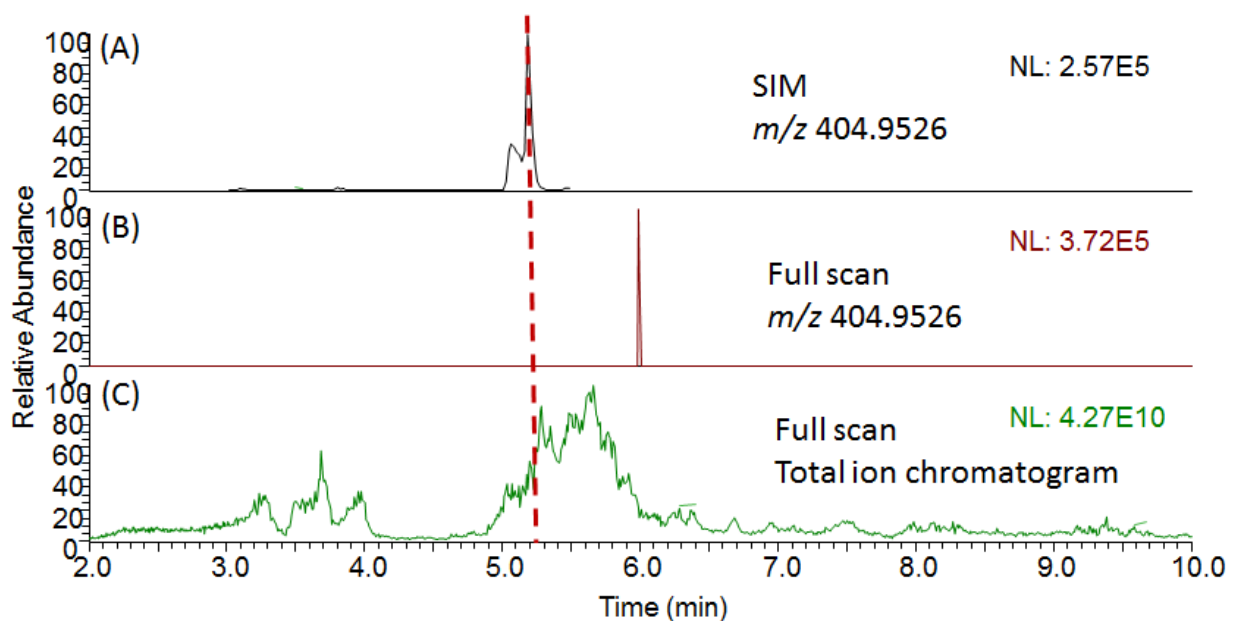


Fig. S6. Comparison of the SIM mode and full scan mode for OH-TBB analysis in dust samples. (A) OH-TBB isomers were successfully detected using SIM mode when extracted the ions at 10 ppm window. (B) OH-TBB could not be detected under full scan mode when extracted the ions at 10 ppm window. (C) Total ion intensity in negative ion mode and comparison to OH-TBB intensity.

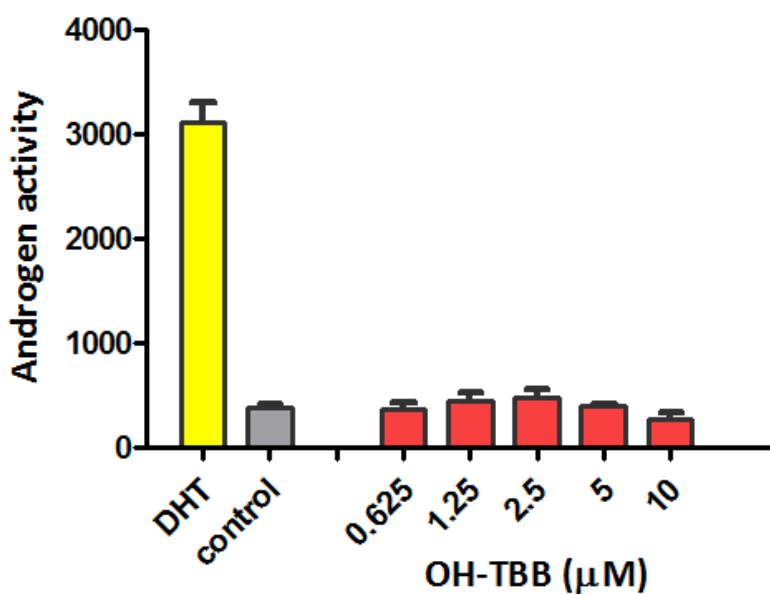


Fig. S7. Androgenic activities of OH-TBB measured by use of *in vitro* bioassay. Activity is presented as absolute response. Exposure to dihydrotestosterone (DHT) (1.0 μM) was used as a positive control.

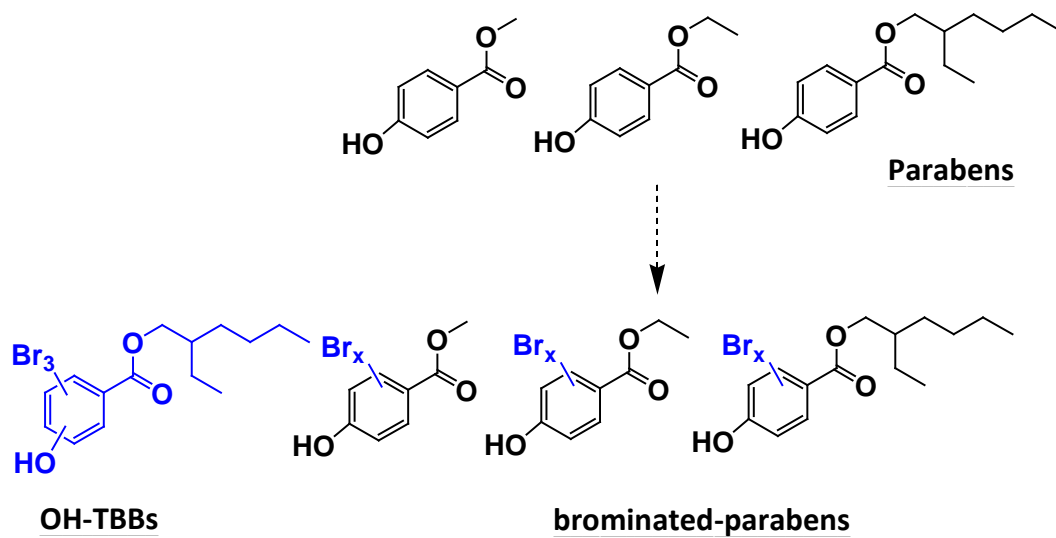


Fig. S8. Comparison of chemical structures of OH-TBB, parabens and brominated parabens.